

Daily ozone vertical profile model built on geophysical grounds, for column retrieval from atmospheric high-resolution infrared spectra

M. De Maziere, O. Hennen,¹ and M. Van Roozendael

Belgian Institute for Space Aeronomy, Brussels

P. Demoulin

Institute of Astrophysics and Geophysics, University of Liège, Liège

H. De Backer

Royal Meteorological Institute of Belgium, Brussels

Abstract. The retrieval of column abundances of atmospheric gases from atmospheric infrared spectra necessarily depends on the choice of the a priori vertical profiles of the atmospheric species involved. Most commonly a standard profile is adopted, and some additional parameter is introduced in the retrieval algorithm for improving the final result. This parameter may be unrelated to geophysical arguments. For the retrieval of ozone columns, it is proposed here to use a model of a priori O₃ vertical profiles which better reflect the real state of the atmosphere at the time and location of the measurement. The model profiles depend on the daily local thermal tropopause height and include a climatological seasonality. The model has been developed for the retrieval of ozone columns from high-resolution Fourier transform infrared (FTIR) solar absorption measurements at the International Scientific Station of the Jungfraujoch in the Swiss Alps. It is demonstrated that the use of the model significantly improves the quality of the spectral fits while minimizing the need for adjusting additional nongeophysical parameters to compensate for atmospheric changes and that it enhances the accuracy of the retrieved O₃ column data. Such is done by comparison of the retrieved FTIR O₃ data with validated independent O₃ data sets from co-located Système d'Analyse par Observations Zénithales and nearby Brewer instruments. Contrary to some other approaches for improving the FTIR O₃ retrieval, the model concept developed here can be applied to O₃ observations at any midlatitude site, and it can be implemented in an operational retrieval procedure.

1. Introduction

High-resolution infrared solar absorption or emission spectroscopy are very powerful techniques for studying the chemical composition of the Earth's atmosphere. Airborne or space observations allow the retrieval of the vertical profiles of observed gases, through the technique of solar occultation or limb emission, respectively [e.g., *Readings*, 1992, and references therein]. Routine ground-based observations are limited mainly to the retrieval of total column abundances.

Actually, most column retrieval algorithms concerned with Fourier transform infrared (FTIR) spectra use a nonlinear least squares fitting procedure between the experimental and corresponding synthetic spectra [e.g., *Park*, 1983; *Niple*, 1980; *Niple et al.*, 1980; *Rinsland et al.*, 1984]. The fit mainly adjusts scalar scaling factors by which the gases' a priori

vertical concentration profiles must be multiplied to obtain the best agreement. However, the vertical distribution determines not only the intensity of the absorption lines but also their line shape via the pressure broadening effect. Thus two critical parameters in the procedure are (1) the effective instrument line shape function and its actual parameters at the time of observation [*Park*, 1982] and (2), the a priori vertical profiles of the target and interfering gases. Erroneous guesses in one or both lead to signatures in the fit residual that often look very similar and therefore are hard to distinguish. In most monitoring efforts, one realistic vertical profile is adopted for all measurement conditions, and one supposes that the instrument is well aligned and therefore that its line function is known sufficiently accurately. One then tries to minimize the fit residual by adjusting either the a priori profile(s) or the effective instrument line shape. The latter one may differ from the theoretical one because of interferogram smearing due to a changing absorbing air mass during the sampling time, intensity errors, etc. [*Park*, 1982, 1983]. For that purpose, many existing codes have introduced one or more additional ad hoc parameters which allow to reduce the fit residual spectrum. Two common parameter choices are (1) a profile upshift or downshift, sometimes called downwelling

¹Now at Paneurolife, Luxembourg.

factor or degree of subsidence (DOS) [e.g., *Toon et al.*, 1992; *von Clarmann*, 1994; *Traub et al.*, 1995; *Abrams et al.*, 1996a, b; *Meier*, 1997; *Notholt et al.*, 1997a, b] and (2) an effective apodisation parameter (EAP) of the spectra [e.g., *Park*, 1983; *Rinsland et al.*, 1984]. The latter parameter does not represent any geophysical variable directly, but it simulates line shape distortions of various possibly unknown origins, including those due to vertical profile shape uncertainties. As shown by *Park* [1983], it may be considered as a mathematical tool for minimizing the fit residual in the hope of getting a retrieved column abundance which better approaches the true unknown value. An EAP smaller (larger) than 1 may be interpreted qualitatively as a positive (negative) DOS, if the DOS parameter D is defined as $V'(z) = V(z(1+D))$; herein z stands for altitude, V for the a priori volume mixing ratio (VMR) vertical profile, and V' for the resulting downshifted (D positive) or upshifted (D negative) profile. D includes profile compression, if positive, or stretching, if negative. EAP equal to 1.0 means that no effective apodisation has been applied, corresponding to the assumption that both the instrument and the atmosphere are modeled correctly and that the molecular spectroscopy calculations are correct.

Techniques are under development for retrieving some vertical profile information from ground-based observations of sufficiently high spectral resolution and quality (signal-to-noise ratio); some test cases have been published already [e.g., *Rodgers*, 1976; *Abbas*, 1979; *Hoell et al.*, 1980; *Taguchi et al.*, 1990; *Stiller et al.*, 1995; *Liu et al.*, 1996; *Pougatchev et al.*, 1996; *Nakajima et al.*, 1997; *Mellqvist et al.*, 1998; *Pougatchev et al.*, 1998; B. J. Connor et al., Retrieval of HCl and HNO₃ profiles from ground-based FTIR data using SFIT2, submitted to *Geophysical Research Letters*, 1998, and references therein]. At the same time, these methods are most beneficial for the improvement of the retrieved columns.

If one aims at an optimized retrieval of ozone column abundances only, one may consider recently published attempts based on an appropriate choice of the a priori vertical profiles, for example, based on the use of climatological profiles (monthly or yearly averages) derived from nearby ozone sonde data [*Murata et al.*, 1997] or on the use of actual nearby soundings and microwave data [*Adrian et al.*, 1991; *Notholt et al.*, 1993; *Rinsland et al.*, 1996; *Wegner et al.*, 1998]. It was shown that such approaches indeed result in ozone column values that are in better agreement with correlative measurements from Dobson observations. The latter approach has the important disadvantage of requiring auxiliary ozone measurements that are quasi simultaneous in space and time, making the FTIR observations of ozone almost redundant. The method of *Bell et al.* [1998] consists in selecting out of a matrix of 225 pre-calculated profiles which take into account tropopause height and diabatic descent, the one that gives the minimum fit residual. Apart from the approach adopted by *Murata et al.* [1997], none of the other ones can be implemented easily in a fast routine retrieval procedure.

Here we will demonstrate that for the same purpose of deriving more accurate ozone column data from ground-based infrared solar absorption spectra in an operational procedure, a better choice of the ozone a priori profile can be derived from daily local tropopause characteristics and a climatological seasonal dependence. The development of this

new model of O₃ a priori vertical profiles and the associated evaluation of the model's value for ozone column retrieval has been carried out for the ozone data recorded by the well-known technique of FTIR solar absorption spectrometry [e.g., *Brown et al.*, 1992] at the International Scientific Station of the Jungfrauoch (ISSJ, 46.5°N, 8.0°E, 3580 m altitude) in the Swiss Alps. The evaluation includes an assessment of the spectral fit quality and intercomparisons of the FTIR ozone column data with correlative Système d'Analyse par Observations Zénithales (SAOZ) and Brewer data. The SAOZ data are obtained from the instrument which is operated also at ISSJ. The Brewer data are obtained at the nearby observatory of Arosa (46.5°N, 9.4°E, 1860 m altitude), only 131 km away from ISSJ.

Figure 1 of *De Mazière et al.* [1998] shows the status of validation of the FTIR O₃ column data at ISSJ with respect to the collocated SAOZ data at the start of this study: one observes a systematic difference between both data sets (based on the standard analyses described in section 2.1), which buries a seasonal variation in it. The SAOZ data at ISSJ can be considered a good proxy for the real ozone column values, as a result of multiple validation exercises and consequent improvements [*Van Roozendaal et al.*, 1998a, b]. Therefore if the new ozone a priori vertical profile model developed here succeeds in eliminating this actually nonresolved discrepancy between the SAOZ and FTIR ozone column data at ISSJ, we are assured of a higher accuracy of the thus retrieved FTIR data: this is the final goal of this work.

Section 2.1 presents the observations and data analysis algorithms used for evaluation of the proposed O₃ vertical profile model. Section 2.2 describes the model development: its concept and technical realizations. The results of the model evaluation are discussed in section 2.3, first, in terms of the accuracy of the retrieved ozone columns (section 2.3.1), and second (section 2.3.2), in terms of the spectral fit residuals. The model relevance is illustrated in section 2.4. Section 3 summarizes the results: benefits, possible uses, and extensions of the new O₃ a priori vertical profile model.

2. Methodology

2.1. Experimental Data

ISSJ is one of the seven stations which together constitute the primary station of the Network for Detection of Stratospheric Change (NDSC) at northern midlatitudes in Europe. This work exploits data from the Bruker 120HR FTIR spectrometer and the SAOZ instrument co-located at the ISSJ. The latter instrument is operated by the Belgian Institute for Space Aeronomy, the former one by the University of Liège. Both instruments and associated data conform to the NDSC quality requirements. The present study is based essentially on the ozone data at ISSJ from January 1995 to the end of October 1997, as such covering nearly three complete years.

In the present study the IR spectra are analyzed for ozone columns in the 3039.18 to 3040.05 cm⁻¹ microwindow, in the O₃ 3ν₃ band; their spectral resolutions vary between 2.85 mK, 4.00 mK and 4.96 mK (1 mK = 0.001 cm⁻¹), depending on the solar zenith angle (SZA) of the measurement and the weather conditions prevailing during the observation. The selection of the spectral window is based on the work of *Hamdouni et al.* [1997] and *Rinsland et al.* [1996]. It satisfies the criteria of

presenting (1) few interferences with other trace gas absorptions and (2) no significant uncertainties originating in the spectroscopic parameters. It is not really optimized for its sensitivity to the temperature and target gas VMR profiles.

The retrieval algorithm used is SFIT version 1.09c [Rinsland *et al.*, 1984] which is based on nonlinear least squares spectral fitting and on the HITRAN92 database for the molecular spectroscopy data [Rothman *et al.*, 1992]. SFIT fixes the VMR profiles of each target gas according to an a priori profile shape, and adjusts only the amplitude, uniformly over the whole altitude range.

In the standard procedure, daily National Centers for Environmental Prediction (NCEP) pressure and temperature profiles for ISSJ are included up to 0.4 hPa (~ 55 km). They are extended to higher altitudes (to 80 km) with the pressure and temperature profiles from the Air Force Geophysics Laboratory (AFGL) U.S. Standard Atmosphere (1976) model [Anderson *et al.*, 1986]. For each absorbing molecule, one fixed standard vertical profile is adopted as the a priori. The molecules which absorb in the selected O₃ microwindow are O₃, CH₄, H₂O and CH₃Cl. As to O₃, the standard SFIT ozone profile is very close to the AFGL U.S. Standard Atmosphere (1976) model referenced above. Besides the adjustment of the ozone concentration scaling factor, the fit procedure also adjusts the CH₄ concentration, a straight-line effective apodisation parameter (EAP), and the baseline of the spectra corresponding to 0% absorption. The latter baseline is assumed to be flat over the range of the spectral microwindow, that is, the baseline parameters are reduced to one scalar value.

The SAOZ spectra (300 to 600 nm) have a spectral resolution of about 1 nm. The differential optical absorption spectroscopy (DOAS) analysis for O₃ is performed in the 470 to 540 nm window. The spectra are inverted towards ozone slant columns. A model atmosphere is required for the calculation of the air mass factor (AMF) which is the ratio of the obtained slant columns to the corresponding vertical columns. Høiskar *et al.* [1997] discussed the dependence of the AMF's seasonal variation on the radiative transfer calculation and the atmospheric data included (pressure, temperature, and O₃ VMR profile): they find a seasonal peak-to-peak amplitude at northern midlatitudes of order 4.6%. In the actually adopted SAOZ analysis, the standard SAOZ algorithm has been used [Goutail *et al.*, 1994], except for the AMF which includes a seasonal variation of order 5.5% peak-to-peak [Lambert *et al.*, 1996]. Hereinafter (section 2.3) the latter seasonality is referred to as the common SAOZ AMF climatology. The reported ozone column data are the average between the morning and evening twilight data, both defined as the average of the vertical columns obtained in the [87°-91°] SZA range. An additional temperature correction has been applied to the SAOZ spectra taking into account the fact that the effective spectral resolution varies with the temperature inside the SAOZ instrument's housing, which fluctuates with the environment's temperature [Van Roozendaal *et al.*, 1998b]. The spectra are corrected before inversion towards slant columns. The resulting O₃ time series can be considered as a good reference for ozone at the Jungfraujoch [Van Roozendaal *et al.*, 1998a, b].

2.2. Ozone Vertical Profile Model Development

2.2.1. Relationships between ozone and tropopause height in the upper troposphere and lower stratosphere.

It is known [Meetham, 1937; Reed, 1950; Vaughan and Price, 1991; Hoinka *et al.*, 1996, and references therein] and it has been verified at the Jungfraujoch [De Mazière *et al.*, 1996] that locally the ozone column abundance is correlated positively with the pressure at the tropopause. It has been shown also that there exists some correlation between the tropopause parameters and the ozone vertical profile, at least in the lowest stratosphere, up to about 22 to 25 km [London, 1985; Danielsen, 1985; Spänkuch *et al.*, 1973].

In this study the daily tropopause altitudes have been derived from a spline fit to daily NCEP temperature vertical profiles above ISSJ, using the standard World Meteorological Organization (WMO) definition of the thermal tropopause [World Meteorological Organization, 1957]. NCEP data are given on 18 pressure levels between 1000 and 0.4 hPa. The spline fit is required to obtain the tropopause with sufficiently high vertical resolution. The frequency distribution of the tropopause heights at the Jungfraujoch sampled over 1995 to 1997 is presented in Figure 1. In this figure, tropopause heights are binned in 1 km wide classes; the horizontal scale indicates the center altitude of the bin. All year round (Figure 1, top), the most frequently occurring tropopause classes above ISSJ are the ones centered around 11 and 12 km, which together represent about 60% of all cases. The distribution is quite narrow, with a full width at half maximum (FWHM) of about three classes. The frequency drops somewhat slower towards the lower tropopause altitudes (< 11 km) than towards the higher ones (> 12 km). Tropopauses lie seldomly

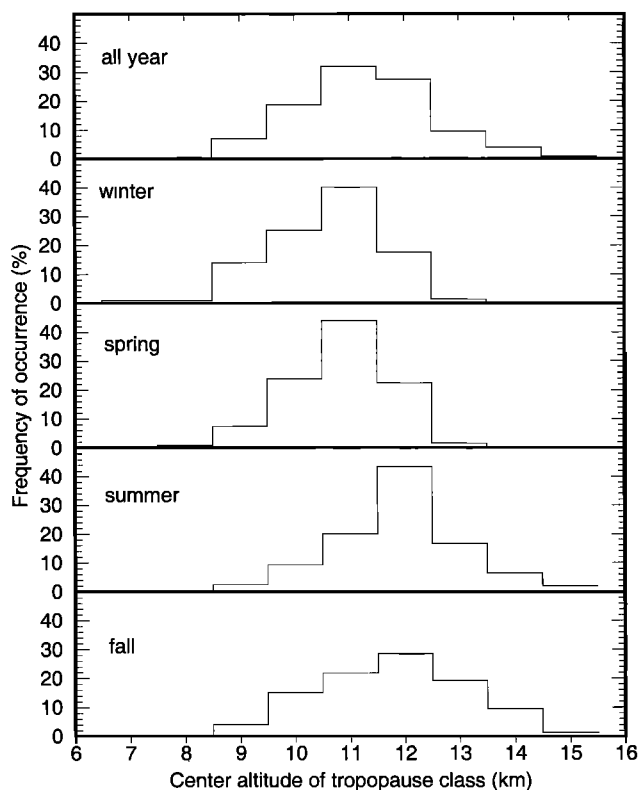


Figure 1. Frequency distribution of tropopause altitudes observed at Jungfraujoch between 1995 and 1997. The occurrence is expressed as a percentage of the total number of observations, year round (top histogram) or per season (lower four histograms). Each season comprises three months, with winter starting on December 1.

below 9 km or above 14 km. We verified that this distribution has little interannual variability. The seasonal variation is illustrated in the lower four panels of Figure 1. Seasons are defined in the same way as in section 2.2.2, that is, 3 months per season with winter starting on the first of December. The central peak of the distribution histogram of tropopause altitudes is more pronounced and is located at 11 km in winter and spring; it is located at 12 km in summer and fall. The distribution is strikingly wider in fall (FWHM of order 3.5 km), while its FWHM is of order 2 km in all other seasons. These studies provide the basic ideas behind the model development discussed hereinafter.

The Royal Meteorological Institute at Uccle (50.8°N, 4.4°E) has one of the longest homogeneous time series of ozone sonde data in Europe. It is one of the ozone records that have been accepted for the determination of long-term trends in the vertical distribution of ozone [Stratospheric Processes and their Role in Climate, 1998]. Ten years of ozone vertical profile data, from 1985 to 1995, have been sorted in nine classes corresponding to tropopause altitudes ranging from (7.0 ± 0.5) km to (15.0 ± 0.5) km, from which an average profile per class has been derived. The classes correspond to the bins in Figure 1. The same WMO definition of the tropopause has been adopted throughout. The thus obtained model relationship between tropopause altitude and ozone vertical profile was discussed by De Mazière et al. [1998]. That discussion included a partial verification of the profile model's validity at the latitude of the Jungfraujoch (46.5°N, 8°E), from a comparison with microwave ozone profile measurements made at Bern (47°N, 8°E). This validity check was extended since over the whole altitude range down to the ISSJ surface level using ozone sonde data recorded at Payerne (46.5°N, 6.6°E), about 150 km W of ISSJ [Staehelein and Schmid, 1991, 1992; P. Viatte, Station Aérologique de Payerne, private communication, 1998]. De Mazière et al. [1998] also highlighted some characteristics of the O₃ profile shapes that are recognized in the O₃ vertical profile model as well as in the experimental data. The altitude of the ozone concentration maximum (AOCM) increases when the tropopause rises, and the value of the ozone concentration at AOCM concurrently decreases. The latter characteristic is associated with the total ozone content decrease with rising tropopause [London, 1985]. Below 15 km the differences between model and experimental profiles get larger than 10% and less constant with altitude. Such is related to the development of a secondary maximum in the ozone concentration vertical profiles, which becomes more pronounced as the tropopause lowers and which is less well captured by the O₃ profile model. This is also consistent with the overall behavior of the standard deviations (1σ) of the model profiles. In all cases, the relative standard deviations are largest indeed, of order 50%, in the altitude range between 10 and 15 km, related to the fact that the ozone concentrations are rather small and that the O₃ profiles have a large gradient with altitude. The smallest relative standard deviations, of order 10 to 15%, are observed in the altitude range of the ozone maximum and above (between 20 and 30 km), where the ozone profiles are rather stable. Also in the middle troposphere around 5 km altitude, the relative standard deviations are small, of order 15 to 20%.

It must be stressed that we are interested solely in the shape of the profile, not in the absolute concentration values. Indeed, the purpose of the O₃ profile model is to provide an

priori estimate of the ozone vertical profile shape, of which anyway the amplitude will undergo a uniform scaling with altitude in the fit procedure of the column retrieval algorithm.

2.2.2. Ozone seasonality. It has been shown earlier that the tropopause changes capture only part of the observed ozone total column changes. De Mazière et al. [1998] show (1) that the tropopause height's seasonal variation is out of phase with respect to the ozone column's seasonal variation observed at ISSJ by SAOZ and that this is due partly to the change of the phase of the seasonal variation of the ozone concentration with altitude [De Mazière et al., 1998, Figure 3] and (2) that the dependence of the ozone vertical profile on the tropopause height as represented by the climatological O₃ vertical profile model discussed in section 2.2.1 cannot on its own reproduce the observed seasonal variation of the ozone column. Such was found also by Steinbrecht et al. [1998a] based on a 27-years time series of ozone soundings at Hohenpeissenberg (47.8°N, 11°E). Two reasons have been identified. As said before (section 2.2.1), the correlation between tropopause height and ozone concentration is limited to the lower stratosphere: above 27 km and in the middle and lower troposphere the O₃ mixing ratio is controlled largely by photochemistry and the influence of tropopause motion becomes negligible [Danielsen, 1985; Steinbrecht et al., 1998a]. And second, tropopause height fluctuations on a day-to-day timescale do not affect the ozone mixing ratio profile at the higher altitudes, for example, up to 27 km, whereas perturbations which last longer such as planetary waves or the annual cycle do [Hoinka et al., 1996; Steinbrecht et al., 1998a].

Therefore a climatological seasonality has been added to the O₃ vertical profile model. First the whole Uccle ozonesonde time series from 1969 to the end of 1997 has been taken into account, and it has been sorted not only according to tropopause height, but also according to season. The long time span of the series guarantees enough data per class to derive a valid climatology, while at the same time being less sensitive to perturbations on a shorter timescale like the O₃ decrease in the period after the Mount Pinatubo eruption, or aberrances due to particular winter conditions. Each season comprises 3 months; the winter season starts on the first of December. Second, the COSPAR International Reference Atmosphere (CIRA) (1986) ozone model [Keating et al., 1990] has been incorporated. The latter model reflects the ozone seasonal (monthly) and latitudinal (per 10° latitude band) variation between 25 and 80 km. It is based on 1978-1982 observations: the average year-round difference of about 35 DU (Dobson Unit; 1 DU = 0.001 atm cm) that has been noticed between the CIRA (1986) ozone columns for 45°N and SAOZ observations at ISSJ is in good agreement with the observed midlatitude ozone trend of about $(0.76 \pm 0.15)\%/yr$ [Jørgensen, 1996]. The CIRA profile data at the ISSJ latitude of 46.5°N have been obtained by linear interpolation between the data for the 40° and 50°N latitude bands. For combining both the Uccle and CIRA sets of ozone profile data, the Uccle sonde profiles are cut at 25 km altitude, where they are extended to higher altitudes by the CIRA (1986) model data for any of the three corresponding months. The CIRA profiles are scaled such that they join the Uccle data at 25 km, which is an ad hoc solution to the previously mentioned overestimation of the actual ozone column in CIRA (1986).

As such, the resulting ozone vertical profile model consists of a set of 108 (= 9x12) profiles, covering the possible

tropopause heights and months of the year. It has been developed for use at ISSJ, but it should be representative of midlatitude Europe in general. It will be called hereinafter the O₃ a priori profile model. Figure 2 is an example set, showing some model profiles for the most frequently occurring tropopause heights, for each season. One recognizes the characteristics recalled above from *De Mazière et al.* [1998], with some seasonal distinctions as to the profile shapes as well as to the behavior of the ozone concentration maximum (Figure 3). These characteristics will be described next, without attempting any geophysical explanation for them, because that is not the subject of this paper.

The increase of AOCM with rising tropopause is most evident in winter and spring. The less systematic relationship observed in summer and fall originates in the fact that for these seasons the peak in the ozone profile is wider vertically, and therefore the location of the ozone maximum is less precise. The value of the ozone concentration maximum decreases with increasing tropopause altitude for all seasons. There is a remarkable difference of about 20% between the higher concentrations in winter and spring, and the lower ones in summer and fall. This behavior remains quite similar if the seasonal cycle is divided in only three seasons (January - April, May - September, and October - December) as suggested by *Spänkuch et al.* [1973, and references therein]. The observed seasonal concentration differences are consistent with the fact that the AOCMs in winter and spring are lower than the ones in summer and fall. The ozone secondary maxima which develop at lower tropopause altitudes are most pronounced in summer and spring.

From Figure 2 it is evident also that the ozone vertical profile shape for a same tropopause altitude changes significantly between different seasons. For example, the profile associated with a tropopause at 11 km develops a

secondary maximum in the spring and summer months, which is hardly present in the other months of the year. At the same time, the ratios of maximum to minimum ozone concentration in the lower stratosphere - upper troposphere change with season, always for the same tropopause height, and so do the relative contributions of the stratosphere and troposphere to the total column (below 25 km). Very similar observations regarding Hohenpeissenberg ozone sonde data have been reported very recently by *Steinbrecht et al.* [1998b]. One concludes from Figures 2 and 3 that the distinct O₃ profile shape variations with season and tropopause height can never be accommodated by a single scaling parameter.

Figure 4 presents an evaluation of the ozone column's seasonal variation at ISSJ during 3 years (1995 to 1997) as predicted by the O₃ a priori profile model. Daily ozone columns are calculated based on the model profile for that month and the locally occurring tropopause altitude, without any concentration scaling; actual daily pressure and temperature profiles from NCEP are used. For comparison, Figure 4 also includes the O₃ column prediction derived from the standard fixed O₃ vertical profile for which the seasonal variation purely originates in the pressure and temperature profiles seasonality. The local SAOZ observations are plotted for reference. Each data set was fitted with a sine curve which is included in the figure. One sees that the predictions based on the O₃ a priori profile model get close to the SAOZ data. There is a small phase lag between both of less than 1 month but the mean values and the amplitudes of the seasonal variations agree quite well. This stands in sharp contrast to the situation based on the standard profile, of which the seasonal amplitude is too small by a factor of 2.

Therefore we expect that the implementation of our new O₃ a priori profile model in the FTIR spectral fit procedure will greatly improve the retrieval of the ozone data and that it will

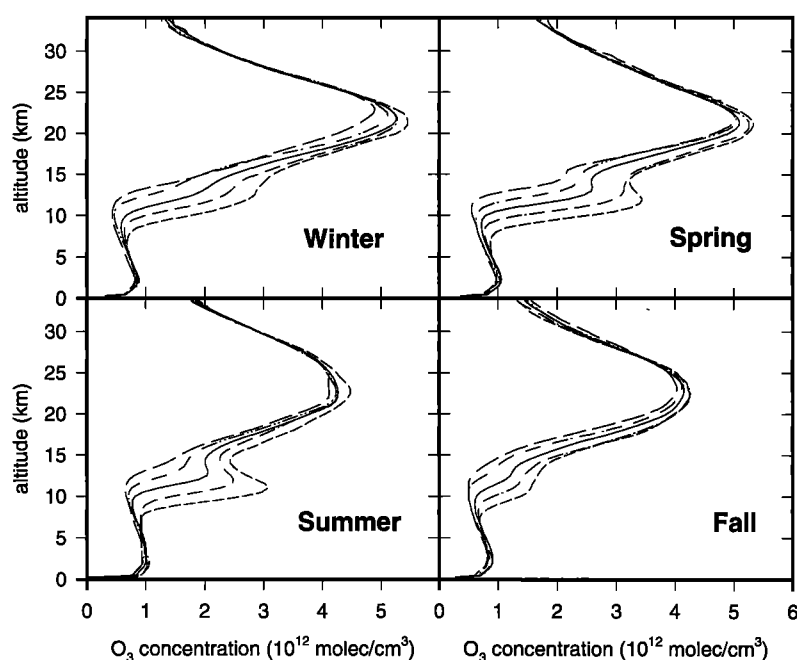


Figure 2. Example set of profiles from the O₃ versus tropopause seasonal profile model. Most frequently occurring tropopause heights are 11 km (solid line) and 12 km (dash-double-dotted line); other curves correspond to a tropopause altitude of 10 km (dash-dotted line), 9 km (short-dashed line), and 13 km (long-dashed line).

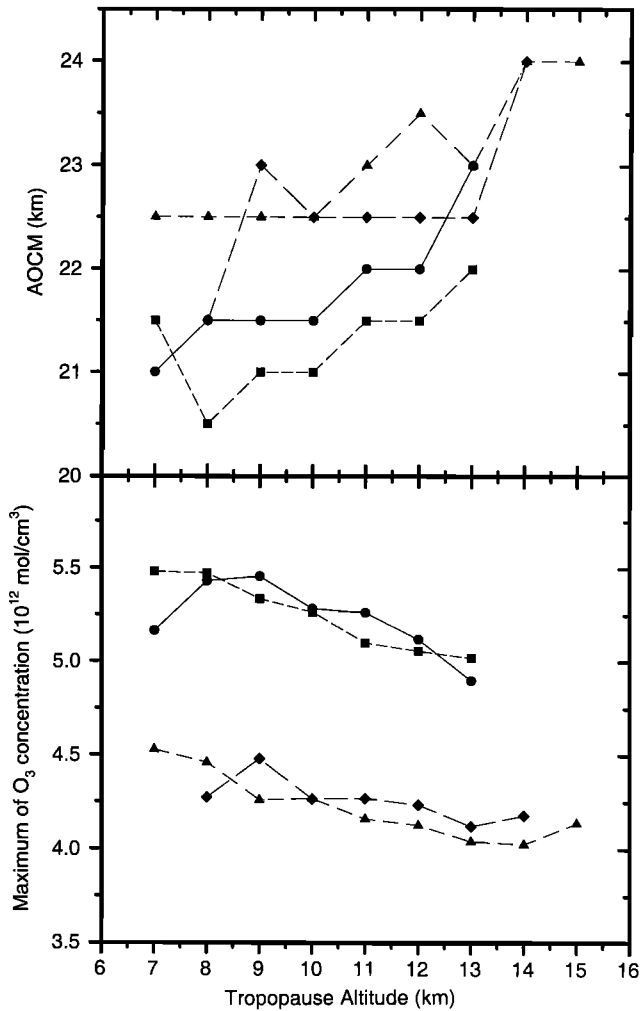


Figure 3. Ozone concentration maximum and corresponding altitude (AOCM) according to the O₃ a priori profile model, as a function of tropopause altitude (per class) and season (circles, winter; squares, spring; diamonds, summer; and triangles, fall).

eliminate to a large extent the discrepancy between the FTIR and SAOZ O₃ time series. This will be demonstrated in the next section.

2.3. Evaluation of the O₃ a Priori Profile Model With Regard to FTIR O₃ Column Retrieval

The ISSJ Bruker IR O₃ spectra for 1995 to 1997 have been analyzed with the SFIT algorithm, once using the standard single O₃ profile, and a second time using the O₃ a priori profile model; all other parameters have been kept identical in both runs. Hereinafter the first cited run will be referred to as the standard O₃ profile run, the second one as the O₃ a priori profile model run. The role of the EAP has been checked at the same time: with both profile models, retrievals have been made once with the EAP fixed to 1.0, and once with the EAP being adjusted in the fit procedure (EAP free).

2.3.1. Accuracy of the retrieved O₃ columns and the role of EAP. The results as to the retrieved O₃ column data in comparison with quasi simultaneous colocated SAOZ data are summarized in Table 1, Table 2, and Figure 6. In the tables, figure, and following discussions, the relative difference between daily mean O₃ columns obtained from the FTIR spectra analysis on the one hand and from SAOZ spectra on the other hand will be called O₃ relative discrepancy. In most cases, this discrepancy shows an annual sinusoidal variation which originates essentially in the phase shift between the seasonal variations of the different data sets, like the one observed already in Figure 4. Therefore this discrepancy is discussed in terms of the parameters of the sine fit to it, namely, the fitted amplitude and the mean value or offset of the sine. The dispersion of the data is discussed in terms of the standard deviation (1σ) of the residuals with respect to the sine fit.

Before entering the discussion, it must be noticed that the quantitative values related to the standard O₃ profile run and SAOZ AMF climatology (EAP free) cannot be compared directly to the ones that go with Figure 1 of *De Mazière et al.* [1998]. First the actual analysis does not cover exactly the same time period. And second, the SAOZ data have now been

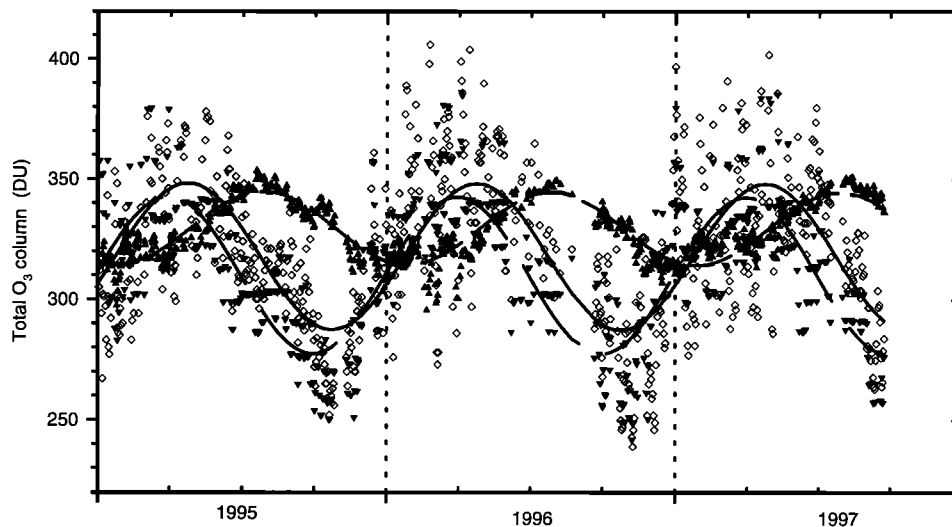


Figure 4. Ozone column annual cycle at ISSJ, based on vertical integrations of the O₃ profiles in the standard model (upward triangles and short-dashed line) and in the new O₃ a priori profile model (downward triangles, long-dashed line). Experimental ISSJ SAOZ ozone data are included for comparison (open diamonds, solid line).

Table 1. Summary of Results of SFIT Runs for 1995 to 1997 ISSJ Bruker Spectra, With the Standard O₃ Profile and the O₃ a Priori Profile Model

		O ₃ Relative Discrepancy (%), With SAOZ Common AMF Climatology		O ₃ Relative Discrepancy (%), With SAOZ AMF From O ₃ a Priori Profile Model	
Sine Fit Parameters		FTIR Analysis With Standard O ₃ Profile	FTIR Analysis With O ₃ a Priori Profile Model	FTIR Analysis With Standard O ₃ Profile	FTIR Analysis With O ₃ a Priori Profile Model
EAP = 1.0	Offset	-3.7 (0.3)	-7.0 (0.3)	-3.2 (0.3)	-6.5 (0.3)
	Amplitude	5.7 (0.4)	2.0 (0.4)	6.2 (0.4)	2.0 (0.3)
EAP free	Offset	-0.1 (0.2)	-0.5 (0.2)	0.3 (0.2)	-0.1 (0.2)
		[-0.5 (0.2)]	[-0.9 (0.2)]		
	Amplitude	3.4 (0.3)	2.6 (0.3)	2.1 (0.3)	1.4 (0.2)
		[3.5 (0.4)]	[2.8 (0.3)]		

EAP (effective apodisation) free or equal to 1.0 means that it is adjusted or not, respectively. The FTIR O₃ columns are compared to colocated SAOZ data, derived either with the commonly adopted AMF climatology (columns 3 and 4) or with AMFs based on the O₃ a priori profile model (columns 5 and 6). Standard errors of the fit parameters are put in parentheses. Comparisons with Arosa Brewer data are mentioned in brackets.

corrected for the instrument's temperature variations, which caused an offset of +2.2% on the mean O₃ value and a seasonal variation amplitude that was smaller by about 0.4% [Van Roozendael *et al.*, 1998b].

To demonstrate that the O₃ a priori profile model developed here indeed improves the FTIR O₃ data, we first looked at the agreement with the colocated SAOZ data derived with the common AMF climatology (columns 3 and 4 in Table 1). As mentioned before, these ISSJ SAOZ data can be taken as a valid reference data set for the ozone abundance above the Jungfraujoch, according to the conclusions from several validation exercises [Van Roozendael *et al.*, 1998a, b]. For confirmation, the FTIR data have been compared to another independent and well-recognized O₃ data set, namely, the Brewer data from Arosa, not corrected for temperature (A. Lehmann, Station Aérologique de Payerne, private communication, 1998).

Next an intercomparison was made with SAOZ O₃ columns derived from a calculation of the AMF according to the same O₃ a priori profile model (columns 5 and 6 of Table 1). The dependence of the SAOZ results on the AMF calculations is illustrated in Figure 5. One observes a slight reduction of the seasonal amplitude of the SAOZ O₃ data in going from the ones based on the common AMF climatology to the ones based on the AMF calculations with the O₃ a priori profile model. The latter data show a much larger variability of course, due to the large short-term tropopause fluctuations. These results are in agreement with the discussions by Høiskar *et al.* [1997] mentioned in section 2.1: differences in the ozone AMF between various model

calculations amount to 1%, and there is a nonnegligible dispersion ($\pm 1.5\%$) of the AMF due to day-to-day changes of the ozone profile. Therefore the purpose of this intercomparison is to check whether remaining discrepancies between FTIR data and SAOZ data based on the common AMF climatology may be attributed to the different O₃ models used in the respective data analyses.

Table 1 shows that in all cases there is significantly less seasonal variation in the O₃ relative discrepancy when the FTIR spectra retrieval algorithm uses the new O₃ a priori profile model instead of the standard profile. First, we discuss the evaluation of the FTIR O₃ columns resulting from a retrieval in which the EAP was adjusted during the fit procedure (EAP free). Considering the FTIR O₃ data obtained with the O₃ a priori profile model in comparison with the SAOZ data based on the common AMF climatology, there is some seasonality left in their mutual disagreement, of order 5.2% peak to peak, which is an improvement by about 25% with respect to the results from the standard O₃ profile run. The mean offset of the FTIR data from the O₃ a priori profile model run with respect to the SAOZ data, although becoming somewhat larger than in the standard case, is smaller than 1%. For both the O₃ standard profile and a priori profile model runs with EAP free, the results of the comparison between the ISSJ FTIR and SAOZ (with common AMF climatology) O₃ data are very similar to the ones obtained from a comparison between the ISSJ FTIR and Arosa Brewer data; the latter values are added in Table 1 in brackets. These results are completely consistent with the ones obtained by Van Roozendael *et al.* [1998a]. They prove that the

Table 2. Similar to Table 1, but for the 1 σ Standard Deviation of the Data Residuals With Respect to the Sine Fit

		Residual of O ₃ Relative Discrepancy Relative to Sine Fit (%), With SAOZ Common AMF Climatology		Residual of O ₃ Relative Discrepancy Relative to Sine Fit (%), With SAOZ AMF From O ₃ a Priori Profile Model	
		FTIR Analysis With Standard O ₃ Profile	FTIR Analysis With O ₃ a Priori Profile Model	FTIR Analysis With Standard O ₃ Profile	FTIR Analysis With O ₃ a Priori Profile Model
EAP = 1.0		3.68	3.53	3.97	3.48
EAP free		2.35	2.27	2.57	2.29

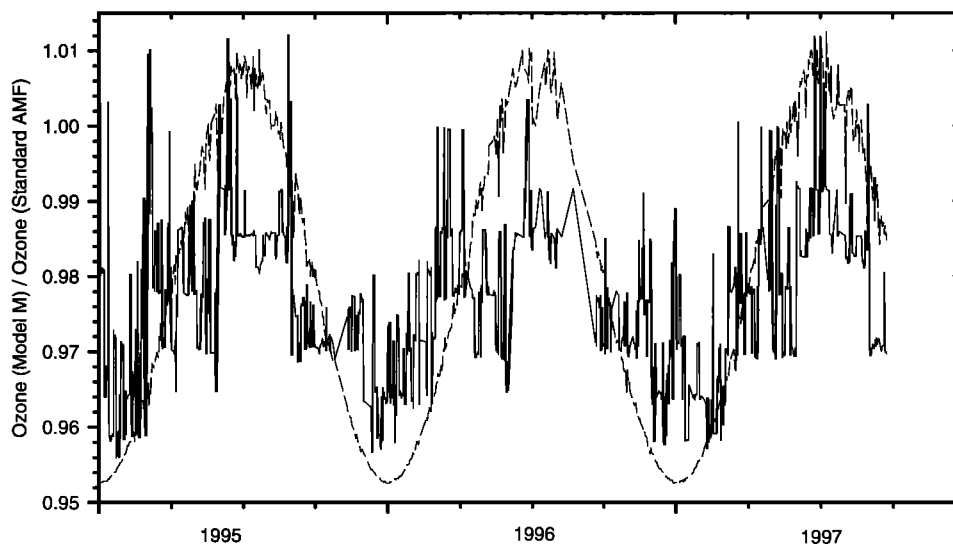


Figure 5. Sensitivity of the SAOZ O₃ column data to the AMF, presented as the ratio of column values relative to the ones obtained with the standard SAOZ AMF [Goutail *et al.*, 1994]. Model M indicates data obtained with either the common AMF climatology (dashed line) or the AMF calculated according to the O₃ a priori profile model (solid line).

implementation of the O₃ a priori profile model leads to an enhanced accuracy of the O₃ columns retrieved from FTIR ground-based solar absorption spectrometry.

However, the agreement between FTIR and SAOZ data can be improved still if the same O₃ a priori profile model is used in both data analyses. In that case one can distinguish some seasonal signal left in the O₃ relative discrepancy, but it is hard to obtain reliable parameters for a sine fit to it, as shown in Figure 6. Therefore the sine amplitude value in the lowest right corner of Table 1 is only tentative. The offset tends to zero. So both data sets come to a very close mutual agreement, as close as the agreement between O₃ data obtained with different UV/visible DOAS spectrometers and well-calibrated Dobson and Brewer spectrophotometers. This demonstrates that the largest contribution to the systematic

discrepancies between FTIR and SAOZ O₃ column data comes from the use of different O₃ VMR profile models in the data analysis.

Second, the EAP is excluded from the fit parameters (EAP fixed). In that case, the use of the O₃ a priori profile model in the retrieval turns out to be even more beneficial. Going from the results from the standard run to the ones from the O₃ a priori profile model run, the mean absolute value of the relative O₃ discrepancy may become larger, but the relative improvement as to the seasonal variation of the discrepancy is higher than with a free EAP. This proves that when using the standard O₃ profile, the EAP is often adjusted in the fit procedure to compensate line shape effects due to real O₃ profile variations. In this respect, it is worth noting that the O₃ a priori profile model run results in about the same amplitude

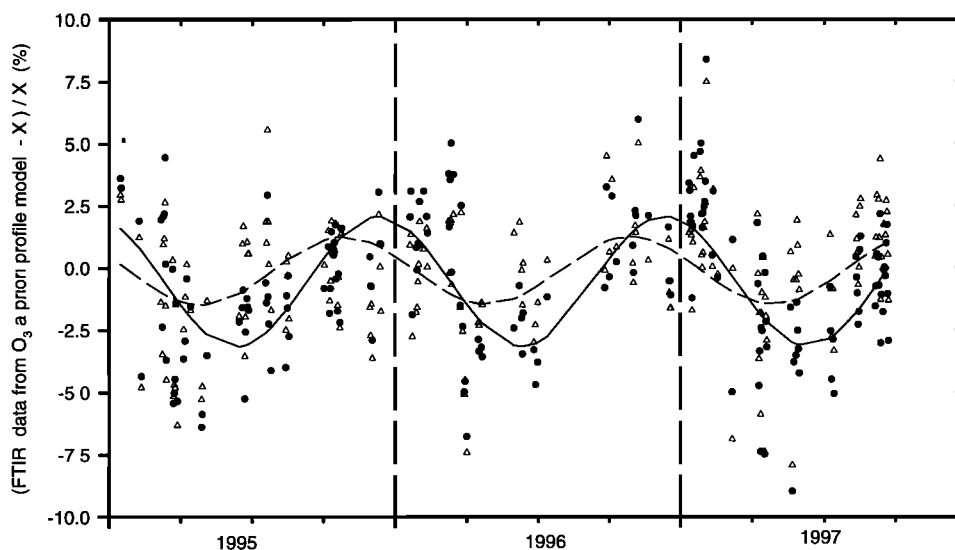


Figure 6. O₃ relative discrepancy in case of SFTIR retrieval using the O₃ a priori profile model, relative to the SAOZ data obtained (1) with the common AMF climatology (solid circles, solid line sine fit) and (2) with AMFs calculated following the same O₃ a priori profile model as the FTIR data (open triangles, dashed line sine fit). The latter sine curve is only tentative.

of the seasonal variation of the O₃ relative discrepancy, whether the EAP is kept fixed or whether it is adjusted in the fit procedure. This is opposed to the results of the standard O₃ profile run, which show a seasonal amplitude of the O₃ relative discrepancy that is far larger with EAP fixed to 1 than with EAP let free.

Thus one can state that the EAP is required in the retrieval procedure as long as one uses the standard O₃ profile, for reducing both the offset and seasonal dependence of the disagreement between FTIR and SAOZ O₃ data. On the contrary with the O₃ a priori profile model, fitting the EAP essentially serves reducing the offset between both data sets and does not impact significantly the seasonal variation in their mutual disagreement.

This role of the EAP is further clarified in Figure 7. Here EAP values obtained for spectra of different spectral resolutions have been converted to the equivalent values for one same spectral resolution (4.96 mK) in order to be intercomparable. When using the standard O₃ profile run, the fitted EAP shows a systematic dependence on the total ozone column. The associated linear regression line has a slope equal to -0.45/100 DU and an offset such that the resulting EAP gets larger than 1 as soon as the total ozone amount drops below 278 DU. Thus EAP values larger than 1 are obtained, which cannot originate in an instrument misalignment only. The O₃ a priori profile model leads to nearly constant EAP values always smaller than 1 (0.7 ± 0.1); the slope of the regression line is only -0.11/100 DU, 4 times smaller than in the standard case. We believe therefore that with the O₃ a priori profile model the EAP is adapted to compensate for a systematic discrepancy between the actual instrument function and its mathematical representation in the retrieval procedure (sinc function times boxcar) or any other systematic discrepancies between calculated and observed spectra, for example, due to uncertainties in the spectral line parameters. Retrievals with a fixed EAP different from 1.0

(e.g., equal to 0.7) confirm that the sine offset can be brought to zero, without modifying the sine amplitude. On the contrary, in the standard O₃ profile run, the EAP adjustment is much more variable, because it also serves compensation for varying atmospheric states.

The behavior of the ozone data on the short term is addressed in Table 2. Here we look at the dispersion of the individual O₃ relative discrepancy data around the seasonal variation. A quantitative measure thereof is the standard deviation of the residual of the individual data relative to the sinusoidal fit of the seasonal variation; this is the parameter reported in Table 2. In all cases, the dispersion decreases after analysis of the data with the O₃ a priori profile model, and relatively more if both SAOZ and FTIR data are based on the same O₃ a priori profile model. Again, fitting the EAP further reduces the dispersion. It appears in fact that the adjustment of the EAP accounts for the largest part of the reduction of the dispersion.

To confirm that it is worth taking into account the daily values of the local tropopause, we compared the values reported in Table 1 and 2 for the O₃ a priori profile model and the common climatology for the SAOZ AMF with analogous values obtained using the same O₃ a priori profile model based on climatological tropopause heights instead of daily observed ones. The sine fit parameters remain identical within the uncertainty limits, but the dispersion of the individual relative discrepancies gets slightly worse again: the standard deviation of the residuals returns to 2.35% if EAP is let free, and rises to 3.86% in case EAP is fixed to 1.0.

Thus one concludes that the O₃ a priori profile model is most powerful for capturing vertical profile variations which happen over a timescale of some days, while it is somewhat less effective for representing the very fast fluctuations from one day to another. This is not too surprising because the model of course represents the climatic feature of the day-to-day variations of the ozone versus tropopause relationship. It

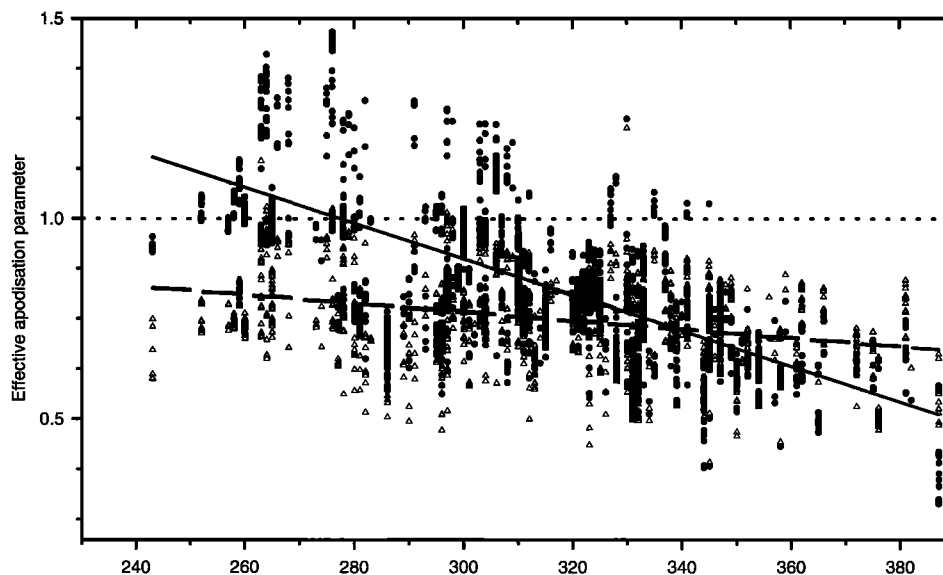


Figure 7. Individual values of EAP (per spectrum) as obtained in the FTIR O₃ retrieval at ISSJ (1995-1997) if EAP is included among the fit parameters. The lines represent linear regression lines through the data points. X axis: value of the total O₃ column obtained from correlative SAOZ measurements. Solid circles and solid line, results from standard O₃ profile run; open triangles and dashed line, results from O₃ a priori profile model run.

may also be related to the physics underlying the model, namely, synoptic-scale meteorological or dynamical perturbations which happen on timescales of a few days [Vaughan and Price, 1991; Steinbrecht et al., 1998a]: the O₃ vertical profile needs some days to adjust to the concurrent tropopause changes. This is reflected in the fact that the correlation between local ozone column and tropopause height gets somewhat worse if focusing on day-to-day fluctuations [Hoinka et al., 1996]. In addition, the ozone profile is influenced by more factors like the temperature profile in the upper troposphere and lower stratosphere, ozone horizontal displacements, tropospheric events, etc., which add a random term to the difference between SAOZ and FTIR data.

2.3.2. Spectral fit residuals. The behavior of the spectral residuals as a function of the choice of the O₃ profiles has been examined, with fixed value of the EAP; the EAP was fixed at 0.7, as this value gave about the most accurate O₃ columns and the best agreement with the experimental data (see previous section). Use of the O₃ a priori profile model leads to a reduction of the spectral fit residuals (difference spectra between calculated and experimental spectra): systematic discrepancies observed in the O₃ absorption lines get smaller or in the best cases nearly disappear. This observation again proves that the O₃ a priori profile model improves the representation of the atmospheric state associated with each spectrum. Figure 8 is a typical example, for September 18, 1997, at 50.46° SZA; on this day, the tropopause height equalled 14.2 km. The top plot shows the superposition of experimental and calculated spectra in the standard O₃ profile run; both spectra are quasi indistinguishable in the O₃ a priori profile model run. The bottom plot shows the respective residual spectra. The

residuum, defined hereinafter as 100 times 1 standard deviation of the residual spectrum over the spectral microwindow considered, decreases from 0.46 in the standard O₃ profile run (dotted line) to 0.22 in the O₃ a priori profile model run (solid line).

From the model profile behavior (see Figure 2) one expects the largest reduction of the residuals to occur for tropopause altitudes far from the most frequently occurring one of about 11 km. This is illustrated in Figure 9 presenting the residuum's reduction, which is defined here as the percent relative difference between the residua obtained in the standard O₃ profile run and in the O₃ a priori profile model run, for all spectra analyzed in 1995, 1996, and 1997. One observes a good correlation between the residuum's reduction and the deviation of the actual tropopause altitude from about 10.5 km. A quadratic regression (solid line) with minimum reduction of order 5% for a tropopause height equal to 10.6 km fits quite well the overall behavior of the individual results (solid circles). The residuum's reduction is marked most prominently for tropopauses higher than 11 km, rising to about 50%. It is also worth noticing that in general significantly larger residua are obtained for spectra taken at large SZA (above 65°), by up to a factor of 5: for these spectra, the residuum's reduction following the implementation of the O₃ a priori profile model is often found to be reinforced.

2.3.3. Summary. In summary, the O₃ a priori profile model indeed addresses most of the O₃ profile changes that are otherwise dissimulated by an ad hoc adjustment of the EAP. Its implementation in the spectral fit procedure generally improves the quality of the spectral fit: smaller spectral residua and more accurate O₃ columns are obtained. Nevertheless, even with the O₃ a priori profile model, an

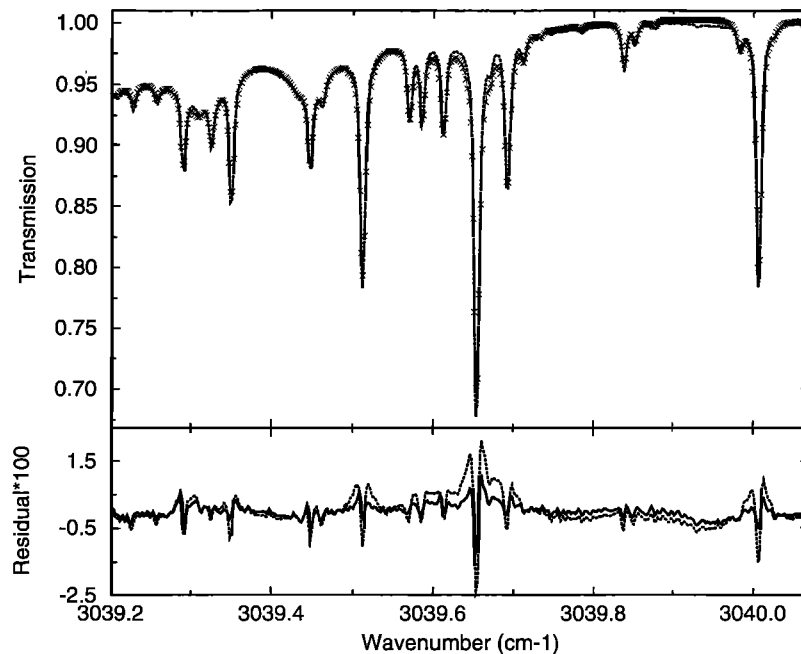


Figure 8. Spectral analysis for September 18, 1997 (SZA = 50.46°, tropopause altitude = 14.2 km). (top) Experimental (cross) and calculated (dotted line) spectra in the standard O₃ profile run. (bottom) Residual spectra (calculated – experimental) for the standard O₃ profile run (dotted line) and the O₃ a priori profile model run (solid line).

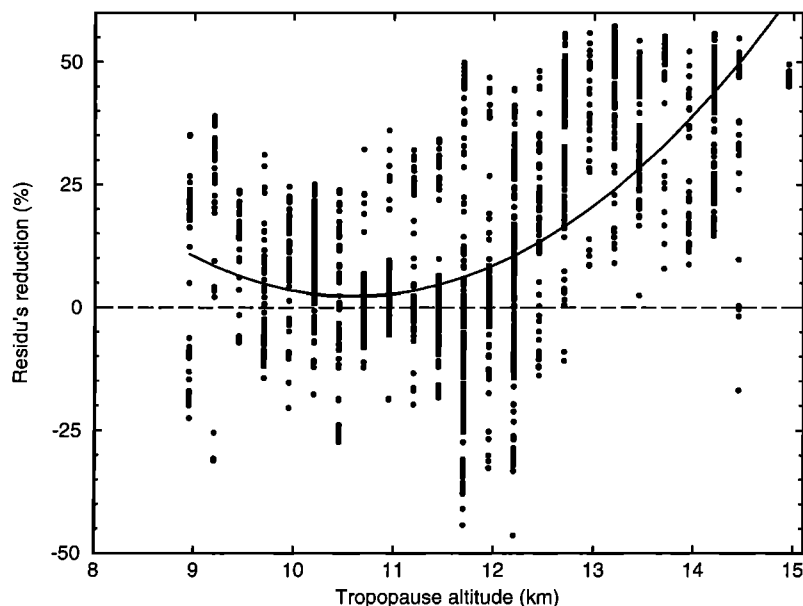


Figure 9. Reduction of residua as a function of tropopause height, for all FTIR spectra considered in the 1995 to 1997 time period (solid circles). The solid line represents a quadratic regression to the individual results. For the definition of residuum's reduction, see section 2.3.2.

additional adjustment of the EAP in the fit procedure is still beneficial to improve the accuracy of the retrieved ozone column amounts, by accounting for some systematic discrepancies left between observed and calculated spectra.

2.4. Relevance of the O₃ a Priori Profile Model

2.4.1. Correlation between tropopause altitude and ozone column. The obtained correlation between the tropopause altitudes and retrieved ozone columns may be a good check for the accuracy of the latter. Therefore we checked whether the correlation between tropopause heights and retrieved ozone columns improved after analysis of the spectra with the new O₃ a priori profile model. This is indeed the case, for the FTIR data as well as for the SAOZ data. For the SAOZ data the degree of correlation $|r|$ rises from 0.70 to 0.77 (for 184 values); the correlation slope changes from (-17 ± 2) DU/km to (-19 ± 2) DU/km. For the FTIR data, the degree of correlation between tropopause altitude and ozone column rises from 0.70 (for 184 values) to 0.72 (for 186 values); the correlation slope changes from (-16 ± 2) DU/km to (-17 ± 2) DU/km. For comparison the correlation was also examined for the independent Brewer O₃ data from Arosa; hereto the tropopause altitudes occurring at the Jungfraujoch were supposed to hold also at Arosa. One finds the following values for correlation slope and coefficient, respectively: (-16 ± 1) DU/km and $|r| = 0.55$ if one takes into account all 562 Brewer data in the 1995 to 1997 time period, and (-20 ± 2) DU/km and $|r| = 0.71$ if the data set is limited to days coincident with the FTIR measurements (131 data). The correlation slopes are not significantly different among each other, and correspond to values around -0.58 DU/mbar taking into account the average relationship between tropopause altitude and pressure. It must be stressed here that the quantitative values of the correlation analyses are very sensitive to the analysis conditions, like the extent of the data set, its seasonal coverage, the time and spatial scales over

which data are compared, etc. This sensitivity can be noticed also from literature and the various values reported at mid-latitude stations [e.g., *Hoinka et al.*, 1996; *Steinbrecht et al.*, 1998a, and references therein]. The important result here is that the data analysis with the O₃ a priori profile model improves the degree of correlation between the retrieved O₃ columns and the corresponding tropopause heights, and that this degree of correlation is about the same as for the independent correlative Brewer data.

2.4.2. Is there a relationship between the O₃ a priori profile model and the DOS parameter? One may wonder whether the implementation of the O₃ a priori profile model cannot be substituted by the introduction of the degree-of-subsidence (DOS) parameter in the retrieval procedure. It was demonstrated by various coworkers in this field and in aircraft and space observations that the addition of such parameter may largely improve retrieval results, while at the same time representing an atmospheric dynamical phenomenon [e.g., *Toon et al.*, 1992; *von Clarmann*, 1994; *Traub et al.*, 1995; *Abrams et al.*, 1996a, b; *Meier*, 1997; *Notholt et al.*, 1997a, b]. One good reason for not adding DOS among the spectral fit parameters is that the number of adjustable parameters increases and therefore also the risk for ending up with mutually correlated variables. To avoid unrealistic results, one may add constraints based on auxiliary geophysical information. The model proposed here immediately introduces such a priori geophysical information into the retrieval procedure, to minimize the number of parameters to be fitted. But we have also verified that the various profiles incorporated in our model in general cannot be derived from each other by just fitting a scaling factor (P_1), a vertical shift (P_2), and a DOS parameter (P_3), as will be shown hereinafter.

Suppose $V_i(z)$ and $V_f(z)$ are VMR profiles of the model. Herein z stands for the altitude and V_i and V_f will be referred to as the initial and final profile, respectively. A set of parameters P_1 , P_2 and P_3 is adjusted through nonlinear least

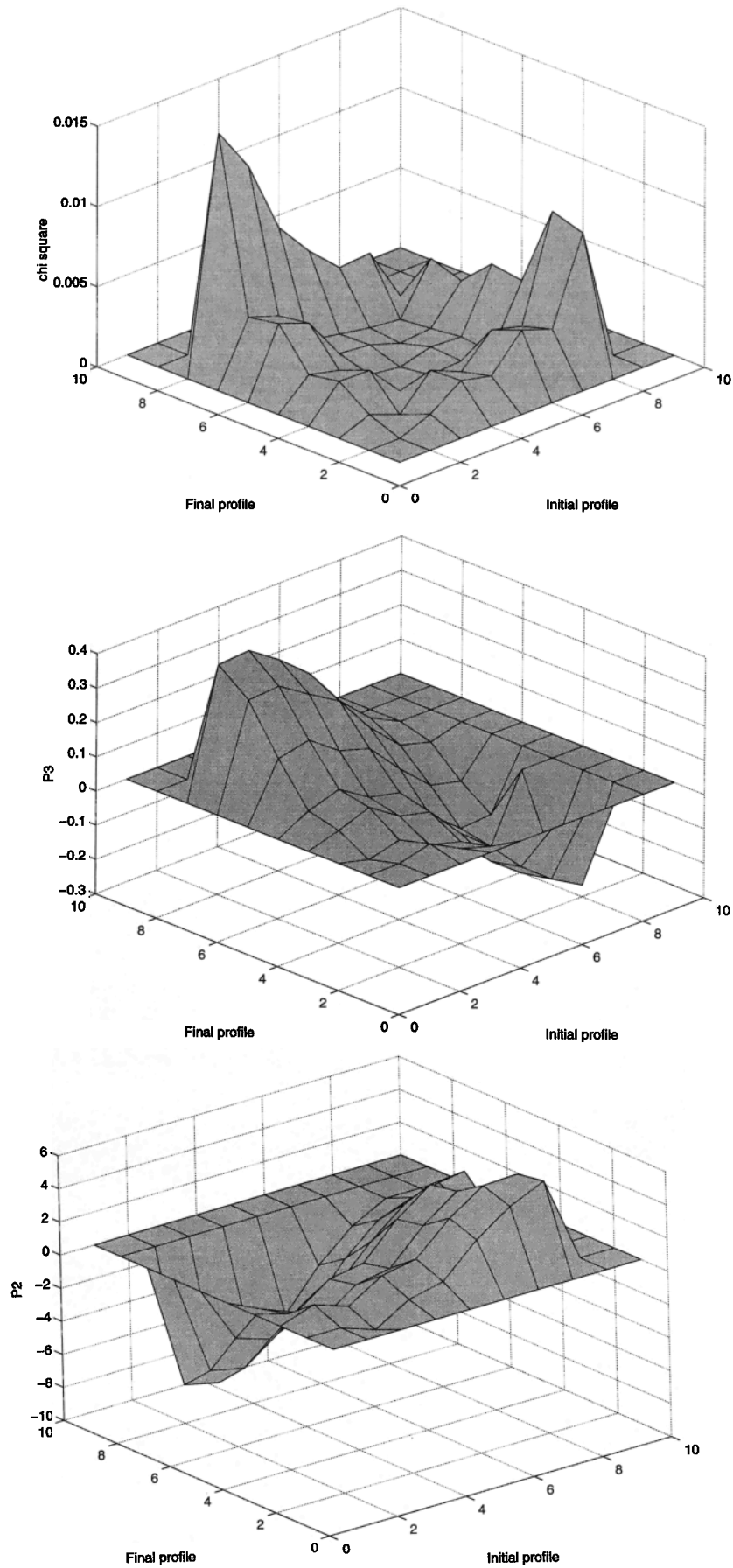


Figure 10. Fit results concerning the transformation from one spring profile of the O_3 a priori profile model to another spring profile, using a scaling factor (P_1), shift (P_2), and DOS (P_3) parameter. Initial and final profiles (X and Y axes) are characterized by the tropopause class number: 0 to 10 correspond to classes centered at 6 to 15 km altitude. Along the Z axis, (a) plot represents the goodness of fit (χ^2) and (b) and (c) plots show the fitted DOS and shift values, respectively.

squares Levenberg-Marquardt fitting to get the best agreement between a transformation of the initial profile $V_i(z)$, according to the expression $P_1 V_i(z(I+P_3)+P_2)$ and $V_f(z)$. Rewriting this expression as $P_1 V_i(z+P_3(z-P_2'))$ with $P_2' = -P_2/P_3$ shows that P_3 represents the degree of subsidence with the shift and stretching of the profile defined with respect to the altitude level P_2' . It turns out from the profile fits that P_2 and P_3 are always opposite in sign, hence P_2' is always positive. With this definition of the parameters, DOS positive (negative) indicates profile compression (stretch) accompanied by profile subsidence (ascent) for altitudes above P_2' and ascent (subsidence) for altitudes below P_2' ; P_2' is a kind of pivot altitude. One cannot expect that the fit should work over the whole vertical altitude range of the profile. As recalled above and confirmed by *Steinbrecht et al.* [1998a] and the experimental observations cited above, this idea holds in the dynamically controlled regime only. Therefore the profile fit was limited to the vertical range between 12 km, the most frequently occurring tropopause level at ISSJ, and 25 km. Figure 10 summarizes the results of such an attempt of transforming spring profiles corresponding to different tropopause altitudes into each other. In going from 0 to 10, one goes from the class of lowest tropopause altitudes (5.5 to 6.5 km) to the one of highest tropopause altitudes (14.5 to 15.5 km). The results agree with expectations from the geophysics behind it. Scaling factors are found close to 1. As mentioned already above, P_3 and P_2 are always opposite in sign. Their signs both change around the diagonal in the XY plane which corresponds to a null operation, that is, the initial and final profiles are identical. The interpretation of the plotted P_3 and P_2 values in terms of the pivot altitude P_2' shows that P_2' is quite constant, with a mean value equal to 20.2 km, and a standard deviation equal to 3.5 km. The profile fits get worse (χ^2 rises) as the tropopause altitudes of initial and final profiles get farther apart from each other.

The result shown in Figure 10 is typical of all cases we checked, that is, of different seasons and of transformations between different seasons, for example, the transformation of a spring profile into a winter profile. Also the mean values of P_2' and their standard deviations are found to be comparable. Nevertheless, in the case of transformations between different seasons, P_2' may take on different values while the quality of the fits tends to be worse for tropopause classes that are close to each other. It also appears that fits get worse by a factor of at least 3 if either the DOS or the shift parameter are excluded from the fit.

Thus it has been demonstrated that the O₃ a priori profile model carries more information than simple profile descent and ascent, as should be expected already from Figure 2 and from the fact that it includes seasonal distinctions. The model is appropriate for the inversion of IR spectral data under usual atmospheric conditions at midlatitude, whereas the DOS concept is probably better adapted to the situation associated with air masses inside or coming from the polar vortex.

3. Conclusions

The O₃ a priori profile model consists of a set of O₃ vertical profile shapes as a function of daily local tropopause height and season. It is developed for providing an a priori profile in the inversion of atmospheric high-resolution infrared spectra, with the aim of improving the accuracy of the retrieved O₃ column, in an operational retrieval scheme.

At the same time the model provides a vertical distribution that better represents the local state of the atmosphere, which reduces significantly systematic discrepancies in the spectral fit residuals. The needed ancillary data are commonly available. The model has been developed and evaluated for use at the International Scientific Station of the Jungfraujoch in the Swiss Alps, but its validity holds at any midlatitude (40°N-50°N) station in Europe. Elsewhere, because of the general validity of the model concept, one may assemble an analogous set of a priori profiles based on the same geophysical characteristics, namely, (1) the correlation between local tropopause height and ozone vertical distribution in the upper troposphere to lower stratosphere (≤ 25 km) and (2) a climatological seasonal variation of the profile at all altitudes. Its use can be extended also to spaceborne nadir-looking experiments. Care must be exercised in polar regions or wherever chemically perturbed conditions are prevailing.

The model evaluation performed here with the SFIT algorithm demonstrates that O₃ column data obtained from ground-based FTIR and SAOZ remote sensing experiments come into very good agreement after implementation of the new model. The agreement between both data sets improves even if the model is implemented in a non self-consistent way, that is, in case the model profiles are used in the FTIR spectral analysis only. In other words, the discrepancies observed in the past between both data sets mainly originated in the absence of sufficient geophysical information regarding the O₃ vertical distribution in the FTIR retrieval procedure. The improvement obtained after implementation of the O₃ a priori profile model is most remarkable if one eliminates the effective apodization parameter from the fit procedure: the seasonality in the discrepancy between both data sets is reduced by a factor of about 3. It is shown also that the residual systematic offset can be explained by systematic uncertainties, for example, in the spectroscopic line parameters or instrument function. Therefore actually, adjustment of the effective apodisation parameter in the fit procedure remains beneficial to compensate for these uncertainties. Of course it should be better in the future to correct for them in a physically appropriate way, by a priori reduction of them. Spectral line shape discrepancies originating in atmospheric changes are now compensated largely by the use of the O₃ a priori profile model, replacing the compensation by the adjustment of the effective apodisation parameter in the standard procedure.

It is shown that the O₃ a priori profile model developed here is able to address atmospheric variations on a short-term scale to some extent, which is not the case with purely climatological models like the one used by *Murata et al.* [1997]. This new model will be a valuable tool for the evaluation of the techniques developed recently for the retrieval of vertical profile information from ground-based high-resolution IR spectra. The main part of the ozone a priori profile model, up to 35 km altitude, is available upon request at the Royal Meteorological Institute of Belgium, Email Hugo.DeBacker@oma.be.

Acknowledgments. The authors thank the FWO -Vlaanderen (Krediet aan Navorsers 1995 - M. De Mazière), the FRFC (contract 2.4533.93), the European Commission (contracts ESMOS-Alps I and II, EV5V-CT93-0348 and ENV4-CT95-0084, respectively, and SCUVS-3, ENV4-CT95-0089), and the OSTC - Services of the Belgian Prime Minister (contracts SMAC, GC/35/002, and ESAC,

CG/DD/01A and CG/DD/01D, in the frame of the Belgian Programme for Global Change and Sustainable Development, and contract ND/35/001) for supporting this research work. Thanks are due to A. Lehmann and P. Viatte, both of the Station Aéronautique of the Swiss Meteorological Institute at Payerne in Switzerland, for providing us with corrected Brewer data from Arosa and ozone soundings from Payerne, respectively. R. Blomme and J. Vandekerckhove of the Royal Observatory of Belgium, J. Granville of the Belgian Institute for Space Aeronomy, and L. Delbouille, G. Roland, C. Servais, and J. Bosselois of the University of Liège (ULG) are acknowledged for their contributions to the observations. The authors are very grateful to E. Mahieu and R. Zander for useful comments and discussions concerning the manuscript. The work would have been impossible without the support from the Jungfraujoch Hochalpine Forschungsstation.

References

- Abbas, M.M., A new inversion method for remote sounding of planetary atmospheres, *J. Geophys. Res.*, **84**, 4387-4392, 1979.
- Abrams, M.C., et al., ATMOS/ATLAS-3 observations of long-lived tracers and descent in the Antarctic vortex in November 1994, *Geophys. Res. Lett.*, **23**, 2341-2344, 1996a.
- Abrams, M.C., et al., Trace gas transport in the Arctic vortex inferred from ATMOS ATLAS-2 observations during April 1993, *Geophys. Res. Lett.*, **23**, 2345-2348, 1996b.
- Adrian, G.P., T. Blumenstock, H. Fischer, L. Gerhardt, T. Gulde, H. Oelhaf, P. Thomas, and O. Trieschmann, Column amounts of trace gases derived from ground-based measurements with MIPAS during CHEOPS III, *Geophys. Res. Lett.*, **18**, 783-786, 1991.
- Anderson, G.P., S.A. Clough, F.X. Kneizys, J.H. Chetwynd, and E.P. Shettle, AFGL atmospheric constituent profiles (0-120 km), *AFGL Tech Rep.*, AFGL-TR-86-0110, 1986.
- Bell, W., et al., Ground-based FTIR measurements of stratospheric trace species from Aberdeen during winter and spring 1993/94 and 1994/95 and comparison with a 3D model, *J. Atmos. Chem.*, **30**, 119-130, 1998.
- Brown, L.R., C.B. Farmer, C.P. Rinsland and R. Zander, Remote sensing of the atmosphere by high resolution infrared spectroscopy, in *Spectroscopy of the Earth's Atmosphere and Interstellar Medium*, edited by K.N. Rao and A. Weber, pp. 97-151, Academic, San Diego, Calif., 1992.
- Danielsen, E.F., Ozone transport, in *Ozone in the Free Atmosphere*, edited by R.C. Whitten and S.S. Prasad, pp. 123-159, Van Nostrand Reinhold, New York, 1985.
- De Mazière, M., O. Hennen, M. Van Roozendaal, P. Demoulin, R. Zander, A. Hamdouni, and A. Barbe, Multiple ozone measurements at the Jungfraujoch. An update after optimised retrieval from FTIR measurements, in *Polar Stratospheric Ozone, Proceedings of the Third European Workshop*, edited by J.A. Pyle, N.R.P. Harris, and G.T. Amanatidis, pp. 532-536, Off. Official Publ. of the Eur. Commun., Luxembourg, 1996.
- De Mazière, M., O. Hennen, M. Van Roozendaal, P.C. Simon, P. Demoulin, G. Roland, R. Zander, H. De Backer, and R. Peter, Towards improved evaluations of total ozone at the Jungfraujoch, using vertical profile estimations based on auxiliary data, in *Atmospheric Ozone, Proceedings of the Quadrennial Ozone Symposium*, edited by R.D. Bojkov and G. Visconti, pp. 25-28, Parco Scientifico e Tecnologico d'Abruzzo, 1998.
- Goutail, F., J.-P. Pommereau, A. Sarkislian, E. Kyro, and V. Dorokhov, Total nitrogen dioxide at the Arctic polar circle since 1990, *Geophys. Res. Lett.*, **21**, 1371-1374, 1994.
- Hamdouni, A., A. Barbe, P. Demoulin and R. Zander, Retrieval of ozone vertical column amounts from ground-based high resolution infrared solar spectra, *J. Quant Spectrosc Radiat Transfer*, **57**, 11-22, 1997.
- Hoell, J.M., C.N. Harward, and B.S. Williams, Remote infrared heterodyne radiometer measurements of atmospheric ammonia profiles, *Geophys. Res. Lett.*, **7**, 313-316, 1980.
- Hoinka, K.P., H. Claude, and U. Köhler, On the correlation between tropopause pressure and ozone above central Europe, *Geophys. Res. Lett.*, **23**, 1753-1756, 1996.
- Høiskar, B.A.K., A. Dahlback, G. Vaughan, G.O. Braathen, F. Goutail, J.-P. Pommereau, and R. Kivi, Interpretation of ozone measurements by ground-based visible spectroscopy: a study of the seasonal dependence of air mass factors for ozone based on climatology data, *J. Quant. Spectrosc. Radiat. Transfer*, **57**, 569-579, 1997.
- Jørgensen, T.S. (Ed.), Stratospheric climatology using UV-visible spectroscopy - 2 (SCUVS-2), final report, contract EV5V-CT93-0334 (DG12 SOLS), part 1, pp. 15-23, Comm. Eur. Commun., Brussels, 1996.
- Keating, G.M., M.C. Pitts, and D.F. Young, Ozone reference models for the middle atmosphere, *Adv Space Res*, **10**, (12)317-(12)355, 1990.
- Lambert, J.-C., M. Van Roozendaal, P. Peeters, P.C. Simon, M.-F. Mérienne, A. Barbe, H. Claude, J. De La Noë, and J. Staehelin, GOME total ozone amounts validation by ground-based observations performed at the NDSC/Alpine stations, in *GOME Geophysical Validation Campaign - Final Results, Workshop Proceedings, Rep. ESA wpp-108*, pp. 115-122, Eur. Space Agency, Paris, 1996.
- Liu, X., F.J. Murcray, D.G. Murcray, and J.M. Russell III, Comparison of HF and HCl vertical profiles from ground-based high-resolution infrared solar spectra with Halogen Occultation Experiment observations, *J. Geophys. Res.*, **101**, 10,175-10,181, 1996.
- London, J., The observed distribution of atmospheric ozone and its variations, in *Ozone in the Free Atmosphere*, edited by R.C. Whitten and S.S. Prasad, pp. 11-80, Van Nostrand Reinhold, New York, 1985.
- Meetham, A.R., The correlation of the amount of ozone with other characteristics of the atmosphere, *Q. J. R. Meteorol. Soc.*, **63**, 289-307, 1937.
- Meier, A., Determination of atmospheric trace gas amounts and corresponding natural isotopic ratios by means of ground-based FTIR spectroscopy in the high arctic, 311 pp., *Reports on Polar Research, Vol 236*, Alfred-Wegener-Institute for Polar and Marine Research, Bremerhaven, 1997.
- Mellqvist, J., B. Galle, X. Liu, B. Connor, M. Chipperfield, J. Urban and M. von Koenig, Retrieval of concentration profiles of HCl and ozone from ground-based FTIR measurements, in *Polar Stratospheric Ozone 1997, Proceedings of the 4th European Symposium on Stratospheric Ozone Research*, edited by N.R.P. Harris, I. Kilbane-Dawe, and G.T. Amanatidis, pp. 708-711, Off. Official Publ. of the Eur. Commun., Luxembourg, 1998.
- Murata, I., Y. Kondo, H. Nakajima, M. Koike, Y. Zhao, W.A. Matthews, and K. Suzuki, Accuracy of total ozone column amounts observed with solar infrared spectroscopy, *Geophys. Res. Lett.*, **24**, 77-80, 1997.
- Nakajima, H., X. Liu, I. Murata, Y. Kondo, F.J. Murcray, M. Koike, Y. Zhao, and H. Nakane, Retrieval of vertical profiles of ozone from high-resolution infrared solar spectra at Rikubetsu, Japan, *J. Geophys. Res.*, **102**, 29,981-29,990, 1997.
- Niple, E., Nonlinear least squares analysis of atmospheric absorption spectra, *Appl. Opt.*, **19**, 3481-3490, 1980.
- Niple, E., W.G. Mankin, A. Goldman, D.G. Murcray, and F.J. Murcray, Stratospheric NO₂ and H₂O mixing ratio profiles from high-resolution infrared solar spectra using nonlinear least squares, *Geophys. Res. Lett.*, **7**, 489-492, 1980.
- Notholt, J., R. Neuber, O. Schrems, T. von Clarmann, Stratospheric trace gas concentrations in the Arctic polar night derived by FTIR-spectroscopy with the moon as IR light source, *Geophys. Res. Lett.*, **20**, 2059-2062, 1993.
- Notholt, J., G. Toon, F. Stordal, S. Solberg, N. Schmidbauer, E. Becker, A. Meier and B. Sen, Seasonal variations of atmospheric trace gases in the high Arctic at 79°N, *J. Geophys. Res.*, **102**, 12,855-12,861, 1997a.
- Notholt, J., G.C. Toon, R. Lehman, B. Sen, and J.-F. Blavier, Comparison of Arctic and Antarctic trace gas column abundances from ground-based Fourier transform infrared spectrometry, *J. Geophys. Res.*, **102**, 12,863-12,869, 1997b.
- Park, J.H., Effect of interferogram smearing on atmospheric limb sounding by Fourier transform spectroscopy, *Appl. Opt.*, **21**, 1356-1366, 1982.
- Park, J.H., Analysis method for transform spectroscopy, *Appl. Opt.*, **22**, 835-849, 1983.
- Pougatchev, N.S., B.J. Connor, N.B. Jones, and C.P. Rinsland, Validation of ozone profile retrievals from infrared ground-based solar spectra, *Geophys. Res. Lett.*, **23**, 1637-1640, 1996.
- Pougatchev, N.S., B.J. Connor, N.B. Jones, and C.P. Rinsland,

- Ground-based infrared measurements of the ozone vertical distribution in the troposphere and lower stratosphere, in *Atmospheric Ozone, Proceedings of the Quadrennial Ozone Symposium*, edited by R.D. Bojkov and G. Visconti, pp. 167-170, Parco Scientifico e Tecnologico d'Abruzzo, 1998.
- Readings, C.J., Limb sounding techniques for environmental monitoring in the Nineties, *Eur. Space Agency Spec. Publ., ESA SP-1140*, 1992.
- Reed, R.J., The role of vertical motions in ozone-weather relationship, *J. Meteorol.*, **7**, 263-267, 1950.
- Rinsland, C.P., R.E. Boughner, J.C. Larsen, G.M. Stokes, and J.W. Brault, Diurnal variations of atmospheric nitric oxide: Ground-based infrared spectroscopic measurements and their interpretation with time-dependent photochemical model calculations, *J. Geophys. Res.*, **89**, 9613-9622, 1984.
- Rinsland, C.P., B.J. Connor, N.B. Jones, I. Boyd, W.A. Matthews, A. Goldman, F.J. Murcray, D.G. Murcray, S.J. David, and N.S. Pougatchev, Comparison of infrared and Dobson total ozone columns measured from Lauder, New Zealand, *Geophys. Res. Lett.*, **23**, 1025-1028, 1996.
- Rodgers, C.D., Retrieval of atmospheric temperature and composition from remote measurements of thermal radiation, *Rev. Geophys.*, **14**, 609-624, 1976.
- Rothman, L.S. et al., The HITRAN molecular database: Editions of 1991 and 1992, *J. Quant. Spectrosc. Radiat. Transfer*, **48**, 469-507, 1992.
- Spänkuch, D., W. Döhler, and H. Kubasch, Statistical characteristics of the vertical ozone distribution in mid-latitudes, *Pure Appl. Geophys.* Vol. 106-108 (1973/V-VII), 1208-1218, 1973.
- Staehelin, J., and W. Schmid, Trend analysis of tropospheric ozone concentrations utilizing the 20-year dataset of ozone balloon soundings over Payerne (Switzerland), *Atmos. Environ.*, **25A**, 1739-1749, 1991.
- Staehelin, J., J. Bader, and V. Gelpke, Trend analysis of the long-term Swiss ozone measurements, in *Proceedings of the Quadrennial Ozone Symposium, Charlottesville 1992*, edited by R.B. Hudson, *NASA Conf. Publ.*, **3266**, 186-189, 1992.
- Steinbrecht, W., H. Claude, U. Köhler, and K.P. Hoinka, Observed increase in tropopause height, Relation to total ozone, in *Atmospheric Ozone, Proceedings of the Quadrennial Ozone Symposium*, edited by R.D. Bojkov and G. Visconti, pp. 175-180, Parco Scientifico e Tecnologico d'Abruzzo, 1998a.
- Steinbrecht, W., H. Claude, U. Köhler, and K.P. Hoinka, Correlations between tropopause height and total ozone: Implications for long-term changes, *J. Geophys. Res.*, **103**, 19,183-19,192, 1998b.
- Stiller, G.P., T. Von Clarmann, A. Wegner, M. Baumann, E. Frank, and H. Oelhaf, Retrieval of tropospheric versus stratospheric partitioning of HCl from ground-based MIPAS FTIR spectra, *J. Quant. Spectrosc. Radiat. Transfer*, **54**, 899-912, 1995.
- Stratospheric Processes and their Role in Climate, Assessment of trends in the vertical distribution of ozone, *SPARC Rep. 43*, SPARC Off., International Ozone Commission/Global Atmosphere Watch, Verrières-le-Buisson, France, 1998.
- Taguchi, M., S. Okano, and H. Fukunishi, Remote sounding of vertical profiles of atmospheric ozone and nitrous oxide with a tunable diode laser heterodyne spectrometer, *J. Meteorol. Soc. Jpn.*, **68**, 79-92, 1990.
- Toon, G.C., C.B. Farmer, P.W. Schaper, L.L. Lowes, R.H. Norton, M.R. Schoeberl, L.R. Lait, and P.A. Newman, Evidence for subsidence in the 1989 Arctic winter stratosphere from airborne infrared composition measurements, *J. Geophys. Res.*, **97**, 7963-7970, 1992.
- Traub, W.A., K.W. Jucks, G.G. Johnson, and K.V. Chance, Subsidence of the arctic stratosphere determined from thermal emission of hydrogen fluoride, *J. Geophys. Res.*, **100**, 11,261-11,267, 1995.
- Van Roozendaal, M., et al., Validation of ground-based visible measurements of total ozone by comparison with Dobson and Brewer spectrophotometers, *J. Atmos. Chem.*, **29**, 55-83, 1998a.
- Van Roozendaal, M., J.-C. Lambert, and H.K. Roscoe, Temperature dependent spectral resolution effects in SAOZ UV-visible spectrometers - Impact on the GOME/ENVISAT validation, in *Seventh GOME & SCIAMACHY Data & Algorithm Scientific Working Sessions, Presentation Material*, pp. 421-438, Eur. Space Agency, ESTEC, Noordwijk, The Netherlands, 1998b.
- Vaughan, G., and J.D. Price, On the relation between total ozone and meteorology, *Q. J. R. Meteorol. Soc.*, **117**, 1281-1298, 1991.
- von Clarmann, T., RAT: A computational tool for retrieval of atmospheric trace gas profiles from infrared spectra, *KfK Rep. 5423*, Kernforschungszentrum Karlsruhe, Karlsruhe, Germany, 1994.
- Wegner, A., G.P. Stiller, T. von Clarmann, G. Maucher, T. Blumenstock, and P. Thomas, Sequestration of HNO₃ in polar stratospheric clouds and chlorine activation as monitored by ground-based Fourier transform infrared solar absorption measurements, *J. Geophys. Res.*, **103**, 22,181-22,200, 1998.
- World Meteorological Organization, Definition of the tropopause, *WMO Bull.*, **6**, 136, 1957.

H De Backer, Royal Meteorological Institute of Belgium, Ringlaan 3, B-1180 Brussels, Belgium.

P. Demoulin, Institute of Astrophysics and Geophysics, University of Liège, 5 Av. De Coïnte, B-4000, Belgium.

O. Hennen, 64B grand Rue, B-6800, Belgium.

M. De Mazière, and M. Van Roozendaal, Belgian Institute for Space Aeronomy, BIRA-IASB, Ringlaan 3, B-1180 Brussels, Belgium. (martine@oma.be)

(Received December 14, 1998; revised May 13, 1999; accepted May 18, 1999.)